JOURNAL OF APPLIED POLYMER SCIENCE VOL. 17, PP. 1771–1784 (1973)

Concerning the Microstructure of dry-RO Membranes

R. E. KESTING, *Chemical Systems Incorporated, Irvine, California 92705*

Synopsis

The microstructure of cellulose acetate reverse osmosis membranes which have been prepared by the Kesting dry process has been elucidated with the aid of scanning and transmission electron microscopy. The *dry-RO* membranes consist of three layers: skin, transition layer, and substructure. The gel morphology of each of these layers originates in its sol precursors within the nascent membrane which manage to survive the sol → gel transition intact. The dense skin layer is composed of aggregates of tiny, slightly ellipsoidal nodules which are believed to be paracrystalline in nature. Immediately beneath the skin lies the transition layer, a narrow band of intermediate density consisting of widely separated closed cells. Below the latter lies the porous substructure which is composed of micrometer-sized, open-celled voids. Because of the size of their substructural voids, dry-RO membranes are able to reversibly undergo wet–dry cycling without densification and loss of permeability.

INTRODUCTION

Since the discovery by Reid and Breton[1] of the high permselectivity of cellulose acetate CA films and the invention by Loeb and Sourirajan[2] of a wet process for the preparation of an asymmetric (skinned) CA membrane, the question of membrane microstructure has been of considerable practical as well as theoretical interest. (The Loeb-Sourirajan wet process is a combined evaporation–diffusion technique in which the fluid casting solution is immersed, after a short evaporation period, into a gelation medium where solvent is exchanged for nonsolvent. The asymmetric wet membranes which result must be annealed to induce permselectivity and maintained wet to avoid densification and loss of permeability.) The wet membrane typically consists of two layers[3]: the "active layer," a thin, dense permselective skin, and the highly permeable porous substructure whose primary function is to serve as a support for the skin.

There are several schools of thought concerning the microstructure of the salt-rejecting layer. Lonsdale et al.[4] and Banks and Sharples[5] hold it to be nonporous and amorphous. Sourirajan,[6] on the other hand, considers the skin to be porous, and a variety of evidence for the presence of crystalline structures has been accumulating.[7–9] A transition zone between the skin and substructure was first distinguished by Gittens et al.[10] but may not be a universal feature. The thick substructure of the wet membrane consists of open-celled voids (0.1–0.5 μm in diameter) whose origin has been related to the emulsoid nature of the solutions from which they are formed.[11–13]

The present study is concerned with dry-RO membranes prepared by the new Kesting dry process. The Kesting dry process is a complete evaporation technique in which the cast solution is allowed to evaporate completely so as to yield an asymmetric permselective membrane without additional fabrication steps.[14] The dry-RO membrane is wet–dry reversible. The microstructure of dry-RO membranes is considered from its origins in the various sol (nascent membrane) phases through the sol → gel transition and to its eventual consolidation within the membrane gel. A comparison is made between the morphologies of wet and dry-RO membranes and the functional consequences of the structural differences between the two. Finally, consideration is given to the effects of the concentrations of polymer and swelling agent in the casting solution upon membrane gel structure.

EXPERIMENTAL

Sol Structure

A mechanical device has been constructed which permits the study of a nascent membrane through its various formative phases from the as-cast sol through the sol → gel transition into the gel state. The apparatus, a nonlinear casting machine, consists of a metal tray and the accessory equipment to mechanically move it according to a prearranged schedule. At the start of the sequence the tray, which contains a milled trough, is filled with casting solution and placed in a covered holding station to prevent desolvation until quiescence obtains. To initiate membrane formation, the tray is drawn from beneath its holding station, very slowly at first, but with constantly increasing velocity. This is accomplished by pulling the tray into the open by means of a leader bar attached to a toggle joint. The tie rods of this joint are moved by a geared linear actuator at a constant velocity along threaded rods in the transverse direction. The effect of this linear transverse motion of the tie rods is to cause their other ends (attached through a single tree to the leader bar), and hence the tray itself, to move at ever increasing velocity. In this way, most of the distance traveled by the tray occurs toward the end of the run so that the majority of the solution is only allowed to desolvate for a short time and, therefore, corresponds to the nascent membrane in its early phases. (That the most profound changes generally occur during the early phases of desolvation is apparent from gravimetric desolvation studies which show that the greatest loss in solution weight occurs during this period.[12]) At the precise moment when the tray completely covers the terminal quenching station, a limit switch is actuated which causes liquid nitrogen to enter the station and impinge upon the bottom side of the tray, thereby causing the nascent membrane to solidify as a glass. At this point the tray contains the entire prenatal history of a dry-RO membrane from the early sol (the last section of the solution to have left the holding station) to the ultimate gel (the first section to have done so). The frozen solution is then lyophilized and examined by SEM microscopy. Deductions as to events occurring on the colloidal level

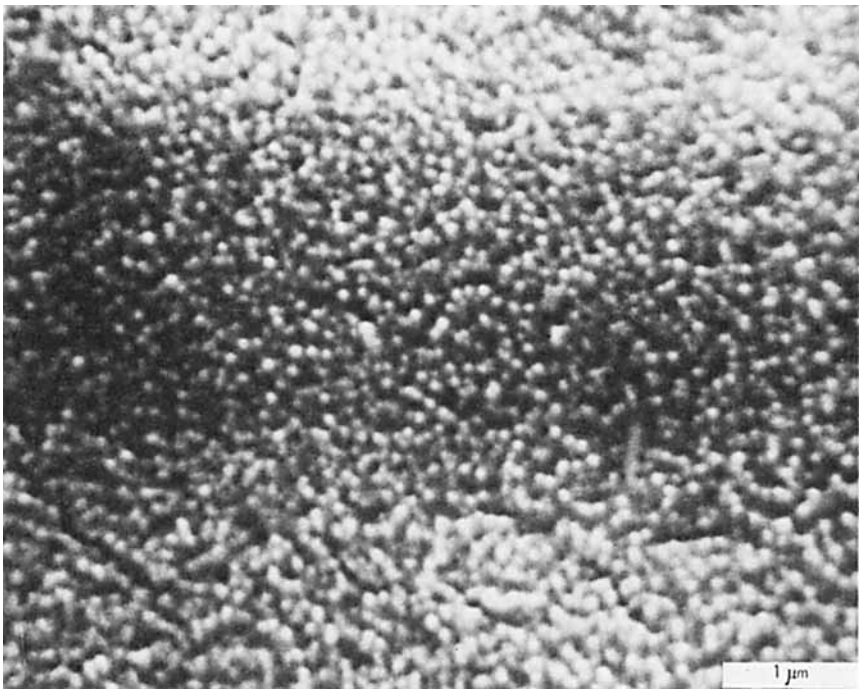

Fig. 1. SEM photomicrograph of spherical nodules in the top surface of a nascent dry-RO membrane.

within the sol during the various stages in membrane formation are then made, based upon a study of the photomicrographs of the "ghosts" of the nascent membrane.[15]

Gel Structure

Electron microscopy of the skin of dry-RO membranes was effected at Scripps Institute by Asunmaa, who together with Schultz,[8] had previously obtained the first EM photomicrographs of details in the skin structure of wet membranes. The skin structure of the dry-RO membrane has since been confirmed in a separate study by Yeh.[16] The dry-RO membrane was etched with 0.6kV argon ions for a period of 1 min. A carbon replica was then formed which was shadowed at a low angle with Au–Pd. After the membrane was dissolved away, an EM photomicrograph was prepared from the replica. For ease of visualization, a converted-contrast print is presented in which the shadows appear as dark areas as in an ordinary photographic print.

SEM photomicrographs of membrane gel structure were prepared according to previously described procedures.[15] Because dry-RO membranes exist in the dry condition, artifact-free photomicrographs are obtained without difficulty.

RESULTS AND DISCUSSION

Sol Structures and the Sol → Gel Transition

An SEM photomicrograph of the top (i.e., the air/solution interface) surface of a lyophilized nascent membrane indicates the presence of spherical droplets (500–1000 A in diameter) at a very early stage in desolvation (Fig. 1). Since the surface of the sol which is exposed to air desolvates more rapidly than interior of the solution, it is not surprising that differences between top and edge views became apparent very early in the membrane formation process (Figs. 2a, 2b). Although the fine

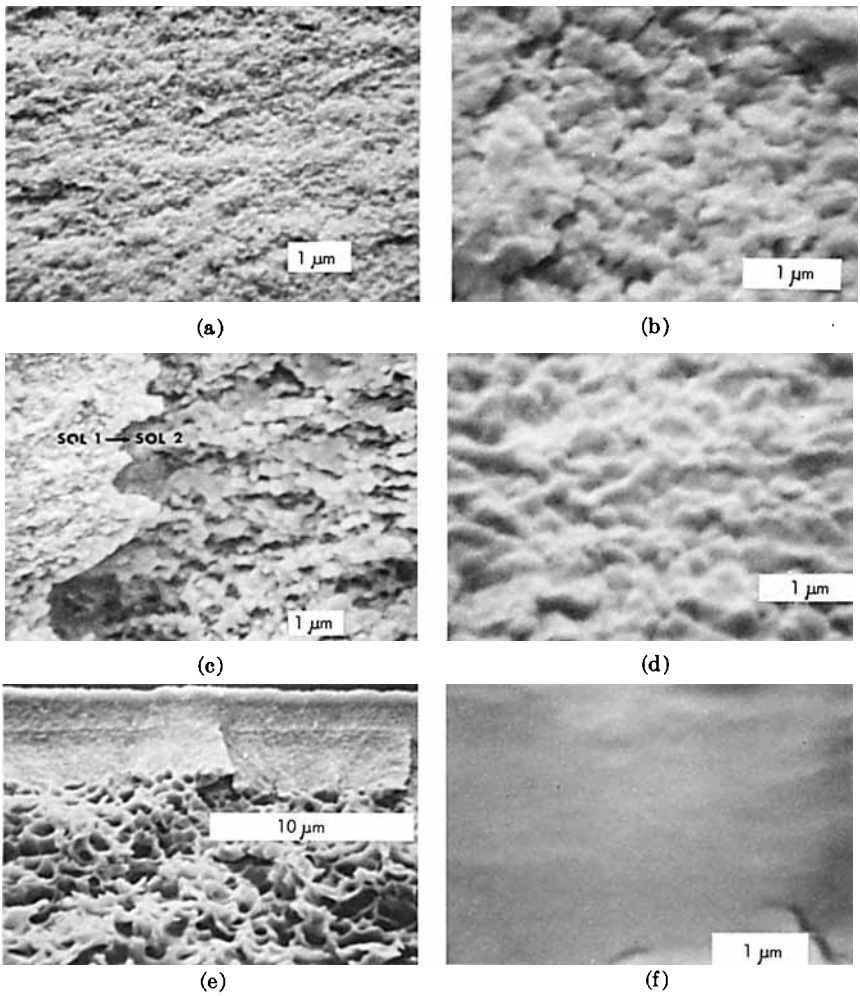

Fig. 2. SEM photomicrographs of lyophilized nascent dry-RO membranes in various stages of formation: (a) edge view early in desolvation; (b) top view early in desolvation; (c) edge view during sol 1 → sol 2 transition; (d) top view during sol 1 → sol 2 transition; (e) edge view after gelation; (f) top view after gelation.

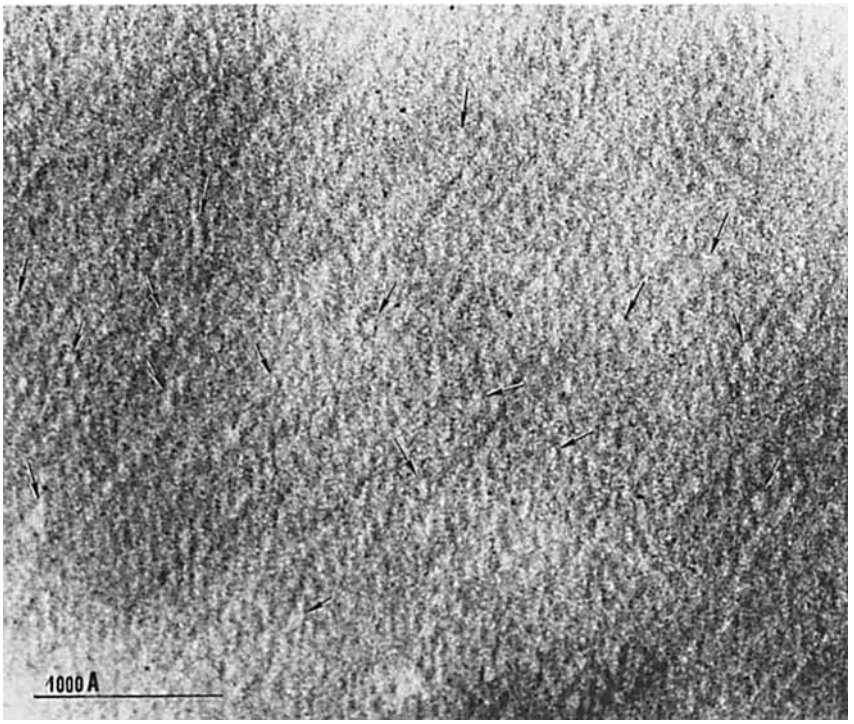

Fig. 3. EM photomicrograph of the ion-etched skin surface of an asymmetric dry-RO membrane.

structure seen above remains evident in the edge view for some time (Fig. 2a), larger (0.3–0.7 μm) structures soon become apparent in the top surface view (Fig. 2b). It thus appears that the individual droplets seen in the edge view have increased in size and agglomerated into spherical aggregates at the top surface. The edge view of a later stage (Fig. 2c) is believed to represent the moment at which the initial sol 1, which is homogeneous at the colloidal level, is transformed into the colloidally inhomogeneous sol 2. (In flasks of solution which have been allowed to desolvate to an extent equivalent to that of the nascent membrane at this stage, a clear solution becomes turbid at this juncture.) This phenomenon is believed to correspond to the appearance of two interdispersed liquid phases previously referred to by Helmcke,[11] Maier,[12] and the present author.[13] The consolidation of the spherical droplets in the various sol phases (2b, 2d) continues gradually until the individual droplets are no longer visible in the finished gel (2f). Substructural consolidation likewise occurs both prior and subsequent to gelation, although to a lesser extent than in the skin (Fig. 2e).

The striking correspondence between the droplet ghosts seen here and the nodules found by Schultz and Asunmaa[8] in their electron photomicrographs of ultrathin and wet membranes of CA is believed to be more than coincidental and indicates the appearance of spherical structures at an early

stage in the prenatal history of dry-RO membranes. The possibility that the structures discussed here might be artifacts has been considered and dismissed. Even in the extremely unlikely event that these nodules are formed as the result of cold quenching and/or lyophilization, the presence of spherical droplets in the sol which are susceptible to conversion into solid nodules in the gel state is now certain.

Membrane Gel Structure

EM photomicrographs of the ion-etched skin surface of a dry-RO membrane clearly illustrate the presence of nodules very similar, but not identical, to those previously found in the skin of wet membranes (Fig. 3). The dry-RO nodules appear to be slightly ellipsoidal rather than spherical. Furthermore the long axis (200 Å) of the ellipsoid appears to be slightly greater than the diameter (188 Å) of the spherical nodules described earlier. Such minor differences may be attributable to the utilization of different polymer grades and/or different solvent systems. The quantitative effect of the presence of ellipsoids rather than spheres is difficult to ascertain, but nodule shape will surely influence packing arrangement. The latter will in turn affect the size and shape of the interstices between the nodules and ultimately, the ordering of water encompassed within the interstitial spaces under reverse osmosis conditions.

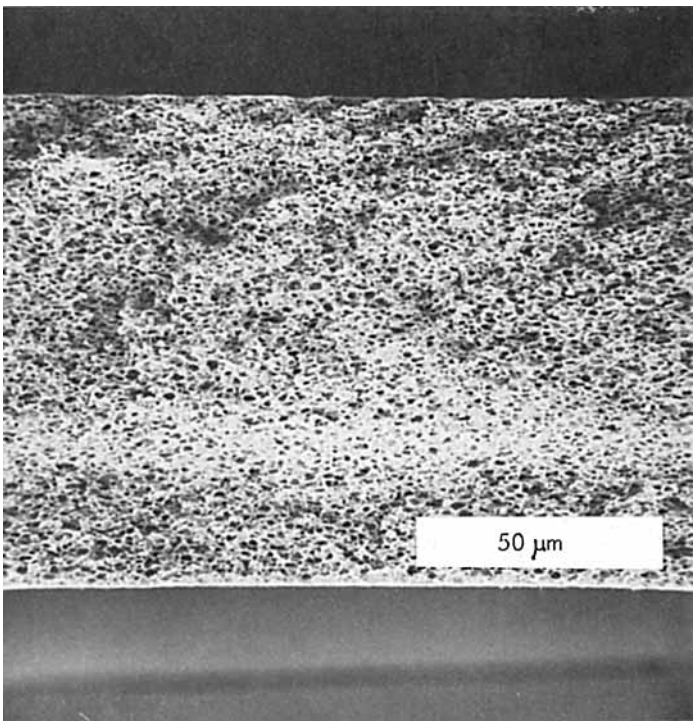

Fig. 4. SEM photomicrograph of the X-section of a dry-RO membrane.

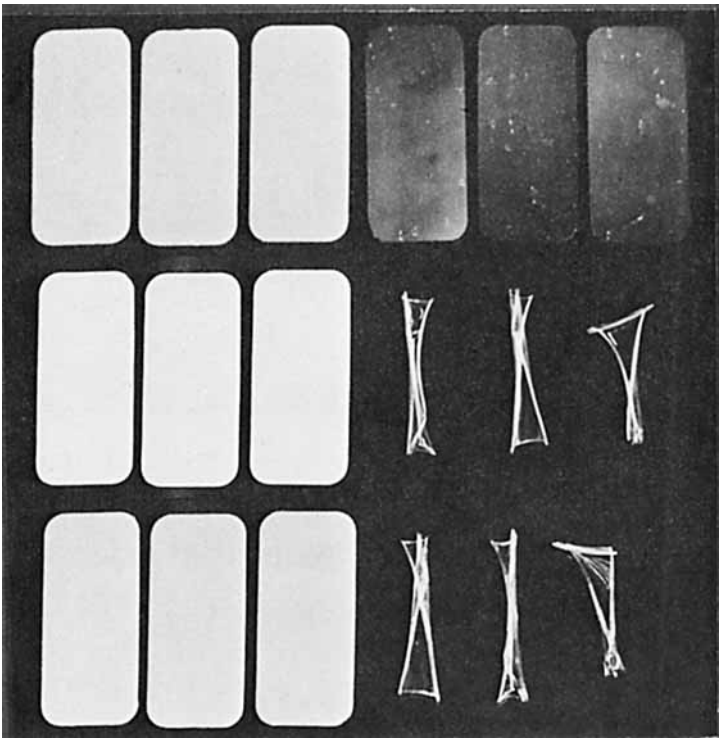

Fig. 5. Comparison of dry-RO (on left) and wet (on right) RO membranes through a single (a) wet → (b) dry → (c) wet cycle.

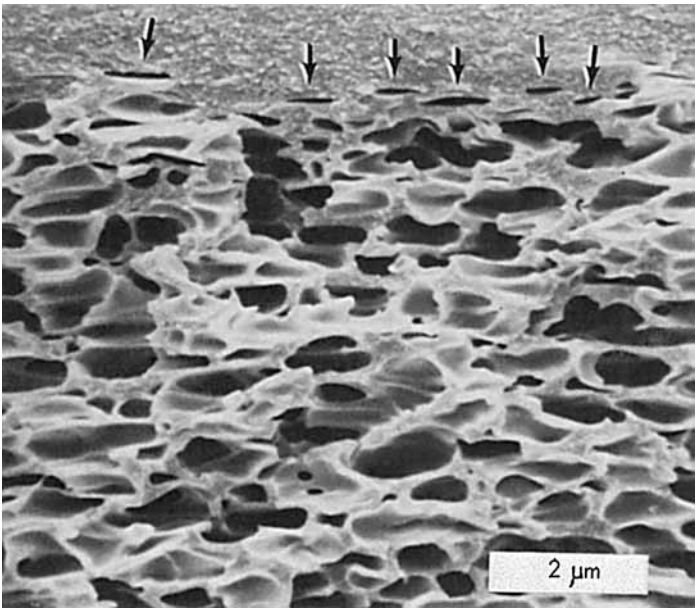

Fig. 6. X-Section of an asymmetric dry-RO membrane showing the skin/substructure interface (arrows denote closed cells).

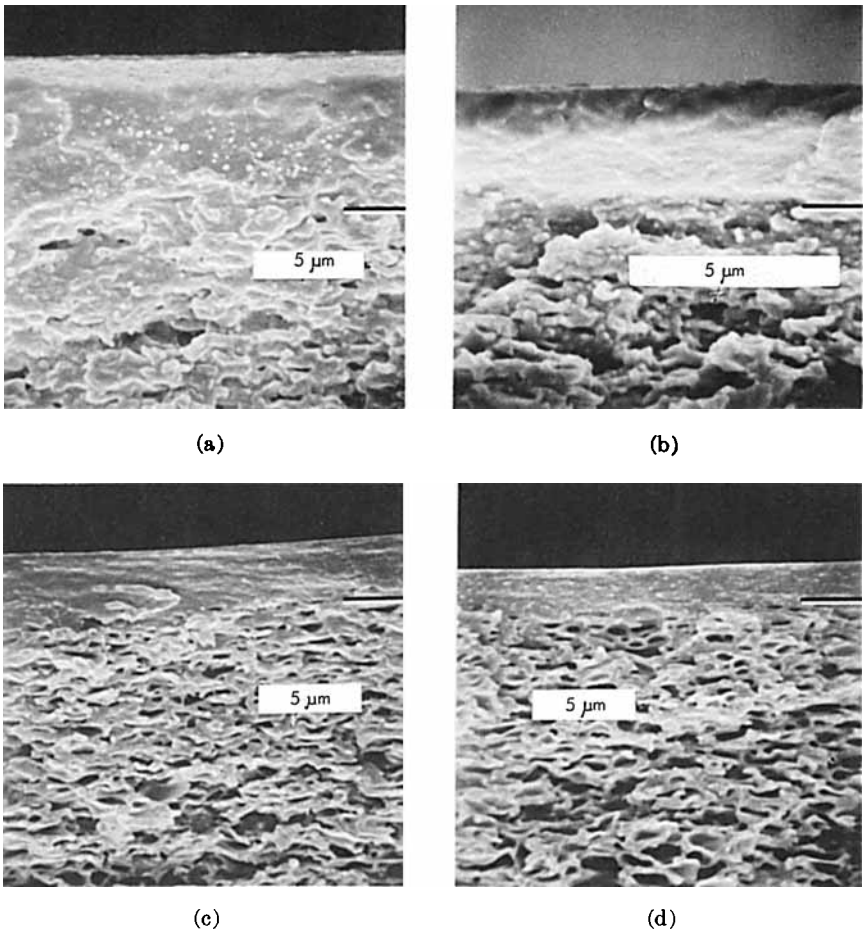

Fig. 7. SEM photomicrographs of skin detail in X-section of dry-RO membranes as a function of swelling agent concentration (lines denote skin/substructure interface): (a) 1 g isopropanol/formulation; (b) 2 g; (c) 3 g; (d) 4 g.

The microscrystalline status of the spherical and ellipsoidal nodules found in the skins of both wet and dry-RO mmebranes is a matter of some interest. Similar structures, termed crystalline nodules by Keith,[17] were first observed by Schoon and Kretschmar.[18] Sjöstrand[19] found them in dense collodion membranes. Yeh and Geil[20] have observed such entities in poly(ethylene terephthalate) and credited them with some paracrystalline order. When annealed at temperatures close to the glass transition temperature, these nodules moved relative to one another and aggregated into clusters about five to ten nodules in diameter. At this point both electron and x-ray diffraction indicate the presence of crystallinity. These phenomena correspond closely to those which occur in the skins of both wet and dry-RO membranes. X-Ray diffraction of unannealed wet CA membranes indicates the absence of crystallinity,[21] whereas annealed

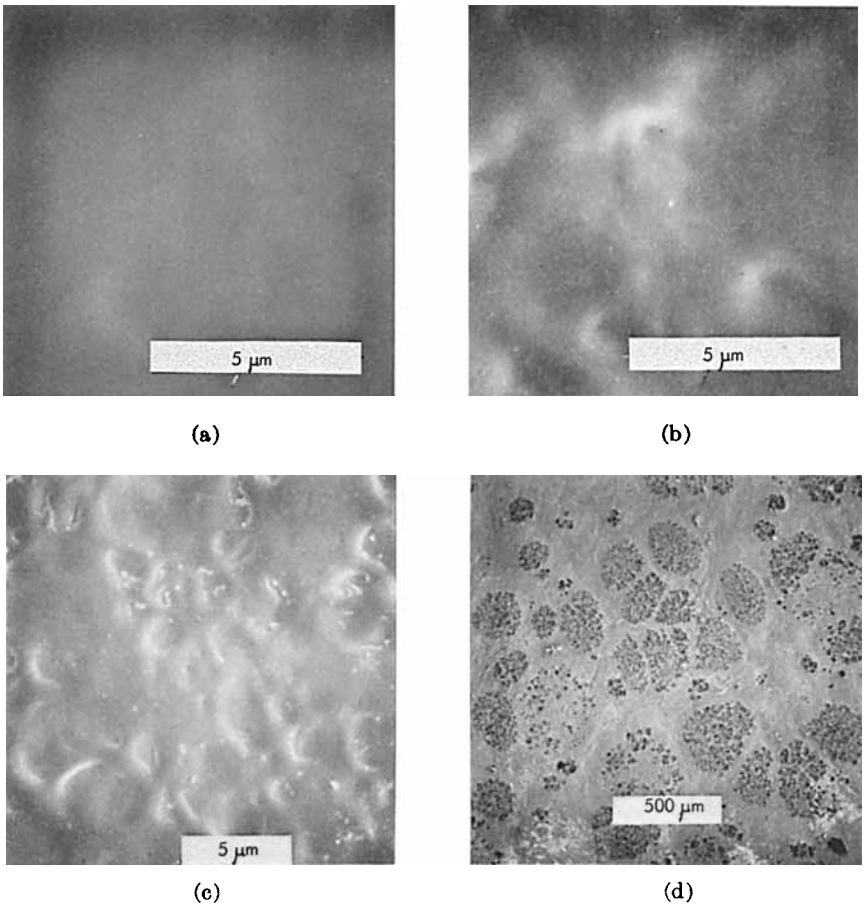

Fig. 8. SEM photomicrographs of the top surface of dry-RO membranes as a function of swelling agent concentration: (a) 15 g isopropanol/formulation; (b) 25 g; (c) 30 g; (d) 35 g.

membranes exhibit a diffraction pattern. The small size of the nodules in unannealed wet membranes apparently precludes their determination by x-ray analysis until they have formed themselves into larger aggregates. Differential scanning calorimetry indicates the presence of some crystalline structure in unannealed dry-RO membranes,[22] presumably because the small nodules have been able, as a result of complete evaporation of solvent, to form larger crystalline aggregates. Ultimately, the problem of the crystalline status of these nodules is concerned with the propriety of considering small ordered regions as crystalline whether or not they are amenable to x-ray analysis. In the opinion of the present author, the nodules in the skins of both wet and dry-RO membranes represent an early phase in the development of crystallinity and as such should rightly be considered at least paracrystalline in nature.

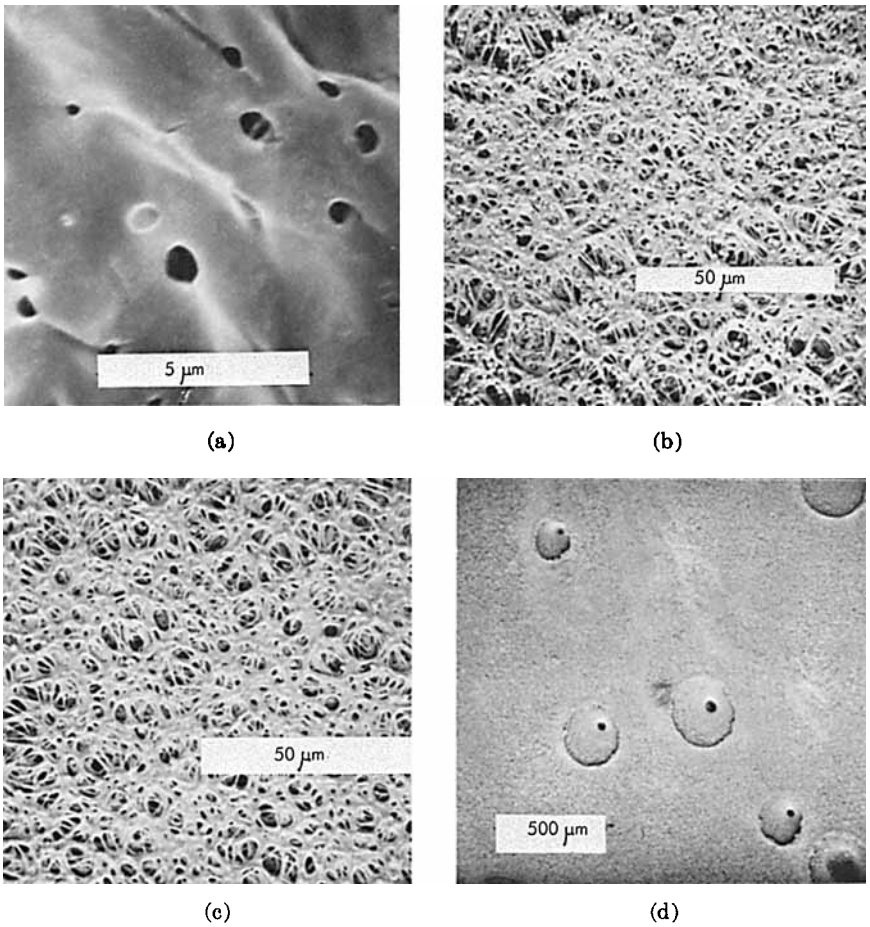

Fig. 9. SEM photomicrographs of the bottom surface of dry-RO membranes as a function of swelling agent concentration: (a) 15 g isopropanol/formulation; (b) 25 g; (c) 30 g; (d) 35 g.

This interpretation is entirely consistent with the known behavior of wet and dry-RO membranes in reverse osmosis. It will be recalled that wet process solutions are allowed only a short evaporation period prior to their immersion into an aqueous gelation bath. Under the reasonable assumption that the paracrystalline nodules observed in the skin of wet membranes are also found in the nascent skin of their sol precursors, they will be immobilized by the extremely rapid solvent exchange which occurs at the moment of immersion into water. This quenching action has a profound effect on the forming skin layer. It freezes the microcrystallites in place before the skin has achieved its maximum density. Since the space between the microcrystallites in the skin of wet membranes in the primary (as quenched) gel condition is relatively large, permselectivity is low or altogether absent. This situation is ameliorated by the addition of a

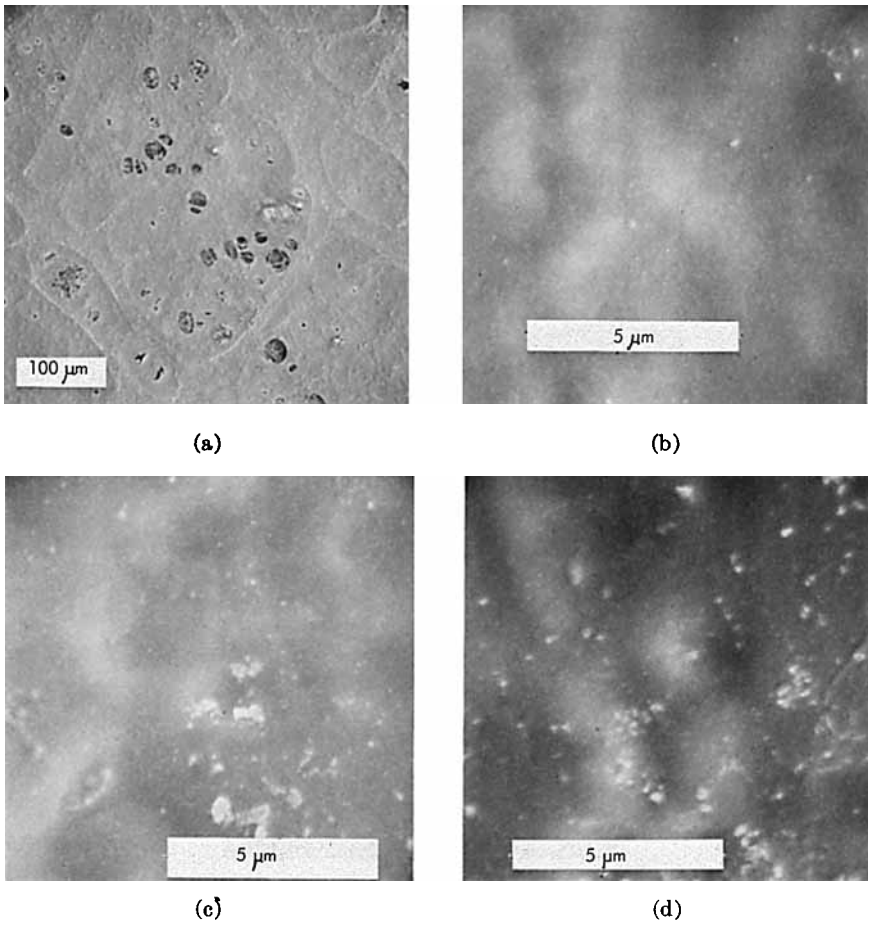

Fig. 10. SEM photomicrographs of the top surface of dry-RO membranes as a function of polymer concentration: (a) 6 g/formulation, (b) 7 g; (c) 8 g; (d) 10 g.

thermal annealing step which forces the microcrystallites together thereby densifying the skin layer. Annealing wet membranes to progressively higher temperatures consequently causes intercrystalline distance to decrease and permselectivity to increase. In the case of dry-RO membranes, complete evaporation of the solvent system allows the microcrystallites to assume a close-packed configuration so that annealing is unnecessary.

SEM photomicrographs of the edge view of dry-RO membranes reveal that the diameter of their substructural voids is in the micrometer range in contrast to that of wet membrane voids which are in the order of 0.1 to 0.5 μm (Fig. 4). This accounts for the optical differences between the two; dry-RO membranes are opaque whereas wet membranes are clear to opalescent. More importantly, however, because of the large size of their substructural voids, dry-RO membranes do not collapse upon drying with

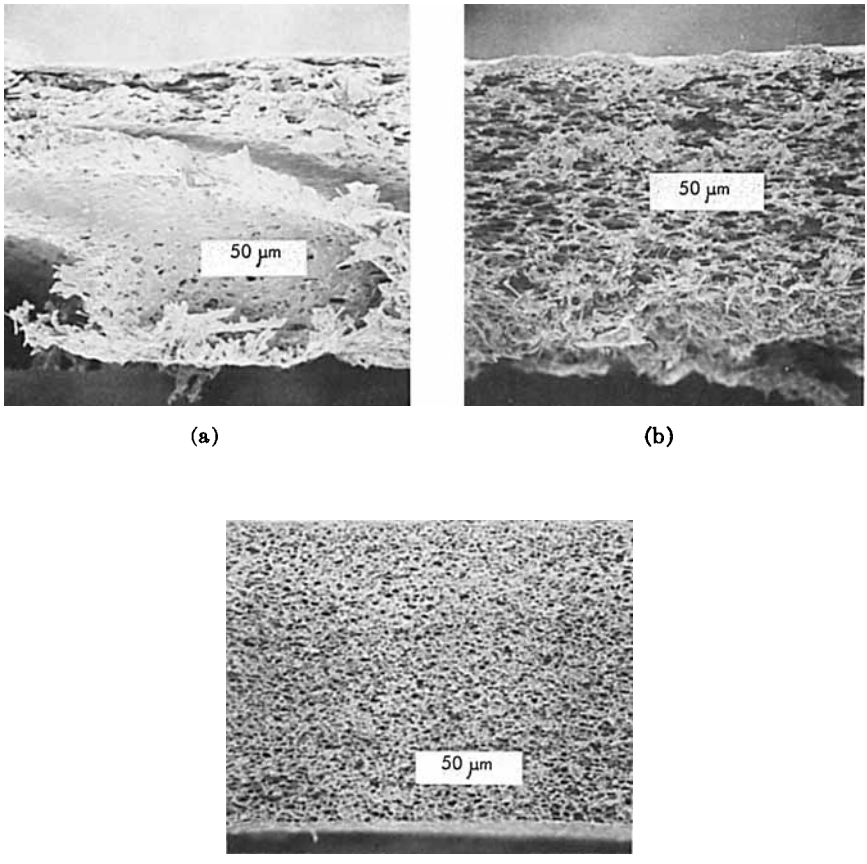

(a) (b)

(c)

Fig. 11. SEM photomicrographs of the X-section of dry-RO membranes as a function of polymer concentration: (a) 7 g/formulation; (b) 8 g; (c) 10 g.

the result that they can be rewet without undergoing structural or functional change (Fig. 5). This is not the case for wet membranes whose small void size results in a substantial internal surface area. The capillary forces which are consequently exerted during drying wet membranes lead, structurally, to irreversible void collapse and membrane densification and, functionally, to a precipitous decline in permeability. Wet membranes which have been brought into a "dry" condition by the glycerol–surfactant exchange procedure are not wet–dry reversible because drying after the surfactant has been leached out inevitably results in membrane densification.[23]

Careful scrutiny of the zone immediately beneath the skin layer of dry-RO membranes reveals that in some, but not all, cases there exists a band which exhibits a density intermediate between that of the skin and that of the substructure proper (Fig. 6). This transition layer appears to consist of closed cell voids and is found in membranes prepared from casting

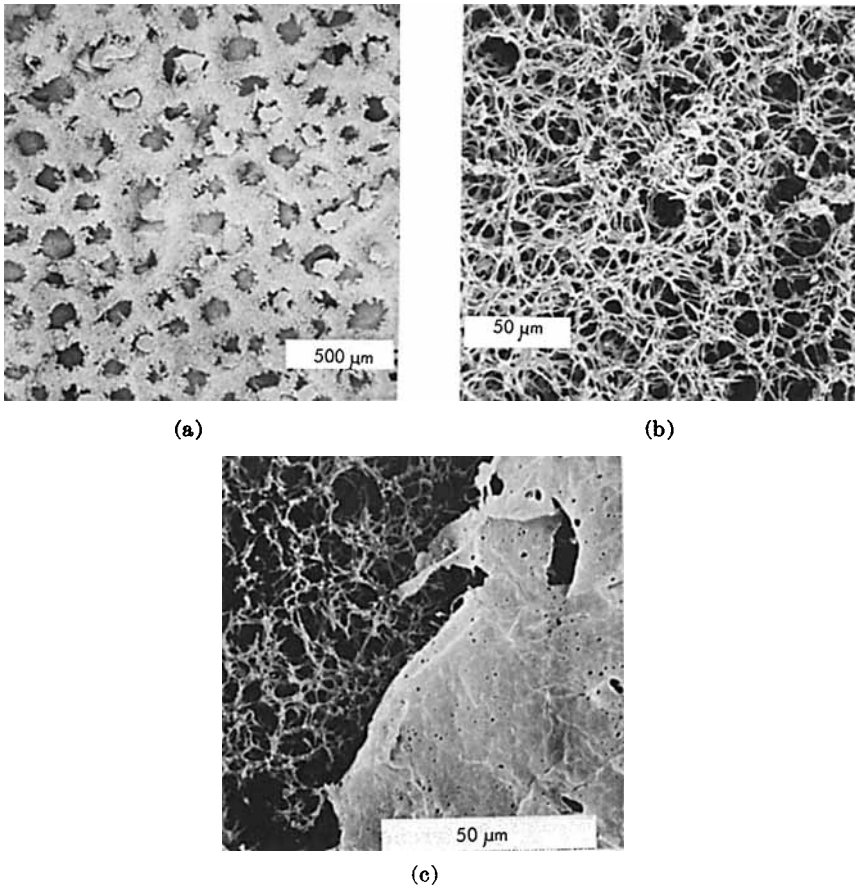

Fig. 12. SEM photomicrographs of the bottom surface of dry-RO membranes as a function of polymer concentration: (a) 7 g/formulation; (b) 8 g; (c) 10 g.

solutions containing low to intermediate concentrations of swelling agent (pore-producing) constituents. Since a solution composed solely of polymer and solvent ordinarily yields a dense film upon drying, it is not surprising that the concentration of pore-producing constituents in multicomponent solutions should determine the extent of deviation of the porous membrane from the dense condition. The closed-cell condition exhibits, of course, a density between that of the dense film and that of an open-celled network. The profound effect of swelling agent concentration upon the structure and function of wet process membranes has been previously considered by the present author.[13,24,25] A closely analogous effect is found in the case of dry-RO membranes. Skin thickness decreases and void volume increases with increasing concentration of swelling agent in the solutions from which the membranes are cast (Fig. 7). At very high swelling agent concentrations, the skin becomes too thin to maintain its integrity over the entire membrane surface (Fig. 8). Macroscopically, the

loss of skin integrity is accompanied by a change in appearance of the skin layer, from a highly reflective surface where the skin is intact to a matte surface where it is not. The bottom surface of the membranes is also affected by swelling agent concentration (Fig. 9). At low concentrations, an irregular bottom surface skin (Fig. 9a) is present which is replaced by the normal substructure at intermediate concentrations (Fig. 9b, c). At high concentrations, substructural integrity disappears and large sinkhole cavities appear (Fig. 9d).

Skin and substructural integrity are also functions of the concentration of polymer in the casting solution (Figs. 10, 11). Below a certain concentration, skin and substructural integrity is impossible (Fig. 10a). Above this concentration, skin integrity results (Fig. 10b–d). However, substructural integrity does not occur until a still higher concentration (Fig. 11). This is presumably due both to the higher polymer concentration and to the more powerful interfacial forces which are operative at the desolvating air/solution interface. Increasing polymer concentration has the same effect on bottom surface structure as does decreasing swelling agent concentration (Fig. 12). Nonintegral structures (Fig. 12a) are replaced at first by normal (Fig. 12b) and then by skinned (Fig. 12c) structures as polymer concentration is increased.

This study was supported by the Office of Saline Water, U.S. Department of the Interior, Contract No. 14-30-2725. The author also wishes to acknowledge the contributions of his colleagues Dr. R. E. Williams in the design and Mr. J. Oakes in the construction of the nonlinear casting apparatus described herein.

References

1. C. E. Reid and E. J. Breton, *J. Appl. Polym. Sci.*, **1**, 133 (1959).
2. S. Loeb and S. Sourirajan, Report No. 60-60, Department of Engineering, University of California, Los Angeles, 1960.
3. H. K. Lonsdale, U. Merten, and R. L. Riley, *J. Appl. Polym. Sci.*, **9**, 1341 (1965).
4. H. K. Lonsdale, in *Desalination by Reverse Osmosis*, U. Merten, Ed., M.I.T. Press, Cambridge, Mass., 1966, Chap. 4.
5. W. Banks and A. Sharples, *J. Appl. Chem.*, **16**, 28, 94, 153 (1966).
6. S. Sourirajan, *Ind. Eng. Chem.*, Fundam., **3**, 206 (1964).
7. R. Kesting, M. Barsh, and A. Vincent, *J. Appl. Polym. Sci.*, **9**, 1873 (1965).
8. R. Schultz and A. Asunmaa, *Recent Progr. Surface Sci.*, **3**, 291 (1970).
9. D. McIntyre and S. Krishnamurthy, paper presented at Third OSW Conference on Reverse Osmosis, Las Vegas, May 11, 1972.
10. G. J. Gittens, P. A. Hitchcock, D. C. Sammon, and G. E. Wakely, *Desalination*, **8**, 369 (1970).
11. J.-G. Helmcke, *Kolloid-Z.*, **135**(1), 29 (1954).
12. K. Maier and E. Scheurmann, *Kolloid-Z.*, **135**, 29 (1954).
13. R. Kesting, *Synthetic Polymeric Membranes*, McGraw-Hill, New York, 1971.
14. Saline Water Conversion Summary Report, OSW, U.S. Dept. Interior, Washington, D.C., 1971–1972, pp. 30–32.
15. R. Kesting, M. Engdahl, and W. Stone, Jr., *J. Macromol. Sci.-Chem.*, **A3**(1), 157, (1969).
16. G. Yeh, private communication, Oct. 1972.
17. H. Keith, *Kolloid-Z. Z. Polym.*, **231**, 430 (1969).

18. T. Schoon and R. Kretschmar, *Kolloid-Z. Z. Polym.*, **211**, 53 (1965).
19. F. Sjöstrand, cited in *Structure and Function in Biological Membranes*, Holden-Day, San Francisco, 1965, p. 633, Figs. 13–32.
20. G. Yeh and P. Geil, *J. Macromol. Sci.*, **B1 235**, 251 (1967).
21. D. Morrow and J. Sauer, Rept. to OSW on Grant 14-01-0001-2130, Aug. 31, 1969.
22. R. Kesting, First Quarterly Report on Contract No. 14-30-2725, Jan. 1971.
23. U. Merten, H. K. Lonsdale, R. L. Riley, and K. D. Vos, OSW Research and Development Report No. 265, 1967.
24. R. Kesting and A. Menefee, *Kolloid-Z. Z. Polym.*, **230**(2), 341 (1969).
25. R. Kesting, in *Cellulose and Cellulose Derivatives*, Vol. 5, Pt. N. Bikales and L. Segal, Eds., Wiley, New York, 1971, Chap. F.1.

Received December 27, 1972